Sun et al. Nanoscale Research Letters (2019) 14:275
https://doi.org/10.1186/s11671-019-3092-x

Nanoscale Research Letters

NANO EXPRESS Open Access

Investigation of energy band at atomic layer deposited AZO/β-Ga_2O_3 ($\bar{2}01$) heterojunctions

Shun-Ming Sun[1], Wen-Jun Liu[1*], Dmitriy Anatolyevich Golosov[2], Chen-Jie Gu[3] and Shi-Jin Ding[1*]

Abstract

The Al-doped effects on the band offsets of ZnO/β-Ga_2O_3 interfaces are characterized by X-ray photoelectron spectroscopy and calculated by first-principle simulations. The conduction band offsets vary from 1.39 to 1.67 eV, the valence band offsets reduce from 0.06 to − 0.42 eV, exhibiting an almost linear dependence with respect to the Al doping ratio varying from 0 to 10%. Consequently, a type-I band alignment forms at the interface of ZnO/β-Ga_2O_3 heterojunction and the AZO/β-Ga_2O_3 interface has a type-II band alignment. This is because incorporating Al into the ZnO would open up the band gaps due to the strong Al and O electron mixing, and the conduction and valence band edges consequently shift toward the lower level.

Keywords: β-Ga_2O_3, Contacts, Intermediate semiconductor layer

Background

Recently, an oxide semiconductor Ga_2O_3 has attracted widespread interests because of its unique characteristics such as the large bandgap, high saturation electron velocity, and high temperature resistance [1]. There are five kinds of isomers for Ga_2O_3: α, β, γ, δ, and ε, where β-Ga_2O_3 can be grown easier and has been studied widely [2]. In particular, β-Ga_2O_3 has a larger breakdown electric field than that of traditional third-generation semiconductor materials, such as SiC and GaN [3]. The n-type conductive properties can be modulated by doping Sn [4] or Si [5]. So β-Ga_2O_3-based devices [6, 7] have broad application prospects in the fields of information technology, energy conservation, and emission reduction. However, β-Ga_2O_3-based devices have a common limitation: the contact between β-Ga_2O_3 and most metals tends to be Schottky because of the large barrier induced by the wide bandgap and finite carrier concentration. In recent years, inserting an interlayer, such as ITO [8] and AZO [9], between Ga_2O_3 and metals is shown to be a valid method to reduce the energy barrier between β-Ga_2O_3 and metal.

Al-doped zinc oxide (ZnO) has gained much attention because of low resistivity and lower fabrication cost than ITO [10]. In particular, the high thermal stability, high mobility, and carrier concentration make it a promising candidate of the intermediate semiconductor layer (ISL) [11]. So far, Al-doped ZnO films can be grown through the following techniques: molecular beam epitaxy (MBE) [12], magnetron sputtering [13], chemical vapor deposition (CVD) [14], and atomic layer deposition (ALD) [15]. Specially, ALD is a renowned method to prepare nano-thickness film which exhibits large area excellent uniformity and unites growth rate per cycle because of the self-limiting surface reaction including the self-limiting chemical adsorption and self-limiting sequential reaction [16]. Moreover, ALD can reduce interface disorder and more precise modulate the Al doping concentration by changing the ratios of growth cycles.

Note that the conduction band offset (CBO) determines the energy barrier for the electron transport, so a smaller CBO is beneficial to form an Ohmic contact. Based on our previous work [17], by increasing Al doping concentration, the Al-doped ZnO film changes from polycrystalline to amorphous nature, and its bandgap widens as well. However, the band offsets of different Al-doped ZnO/β-Ga_2O_3 heterojunctions have not been studied widely. In this work, the ZnO films with

* Correspondence: wjliu@fudan.edu.cn; sjding@fudan.edu.cn
[1]State Key Laboratory of ASIC and System, School of Microelectronics, Fudan University, Shanghai 200433, China
Full list of author information is available at the end of the article

© The Author(s). 2019 Open Access This article is distributed under the terms of the Creative Commons Attribution 4.0 International License (http://creativecommons.org/licenses/by/4.0/), which permits unrestricted use, distribution, and reproduction in any medium, provided you give appropriate credit to the original author(s) and the source, provide a link to the Creative Commons license, and indicate if changes were made.

different Al doping ratios were respectively deposited on β-Ga_2O_3 substrates by ALD. The results show the VBO and CBO are almost linearly dependent on the Al doping ratio.

Methods

The substrates are bulk β-Ga_2O_3 ($\bar{2}01$) and the doping concentration is about $3 \times 10^{18}/cm^3$. The cleaning process for Ga_2O_3 substrates was undergone ultrasonic wash in acetone and isopropanol for each 10 min with repeated three times. Subsequently, the Ga_2O_3 substrates were rinsed with deionized water. Afterwards, the Al-doped ZnO films were grown onto the Ga_2O_3 substrate by ALD (Wuxi MNT Micro Nanotech Co., LTD, China). Three kinds of samples were prepared. Firstly, the undoped ZnO films were grown by ALD with the precursors of Zn $(C_2H_5)_2$ (DEZ) and H_2O at 200 °C. Secondly, the Al-doped ZnO films were carried out by adding one pulse of trimethylaluminum (TMA) and H_2O every 19th cycle of DEZ and H_2O pulsing (denoted as 5% Al doping) at a substrate temperature of 200 °C during ALD. Thirdly, the Al-doped ZnO films of ratio 9:1 (denoted as 10% Al doping) were also prepared. The growth rate of ZnO and Al_2O_3 was 0.16 and 0.1 nm/cycle, respectively. Every kind film included two different thicknesses, i.e., 40 nm and 10 nm for the thick and thin film, respectively. In addition, the β-Ga_2O_3 substrate was used to study the bulk material. Ga 2p, Zn 2p CLs, and the valence band maximum (VBM) were measured by X-ray spectroscopy (XPS) (AXIS Ultra DLD, Shimadzu) and the step of resolution XPS spectra is 0.05 eV. To avoid the surface contamination of the sample during the transfer process from ALD to XPS chamber, Ar ion etching was performed before the XPS measurement. Note that the charging effect can shift the XPS spectrum, and the BE of C 1s peak is calibrated at 284.8 eV to solve the problem.

Results and Discussions

The valence band offset (VBO) of Al-doped ZnO/β-Ga_2O_3 heterojunction can be obtained through the formula as follows [18]:

$$\Delta E_V = E_{Ga\ 2p}^{Ga_2O_3} - E_{VBM}^{Ga_2O_3} - E_{Zn\ 2p}^{AZO} - E_{VBM}^{AZO} - E_{Ga\ 2p}^{Ga_2O_3} - E_{Zn\ 2p}^{AZO} \quad (1)$$

where $E_{Ga\ 2p}^{Ga_2O_3}$ refers to the binding energy (BE) of Ga 2p core level (CL) in bulk β-Ga_2O_3, $E_{VBM}^{Ga_2O_3}$ refers to the BE of VBM in bulk β-Ga_2O_3, $E_{Zn\ 2p}^{AZO}$ refers to the BE of Zn 2p CL in thick Al-doped ZnO films, E_{VBM}^{AZO} refers to the BE of VBM in thick Al-doped ZnO films. The latter $E_{Ga\ 2p}^{Ga_2O_3}$ and

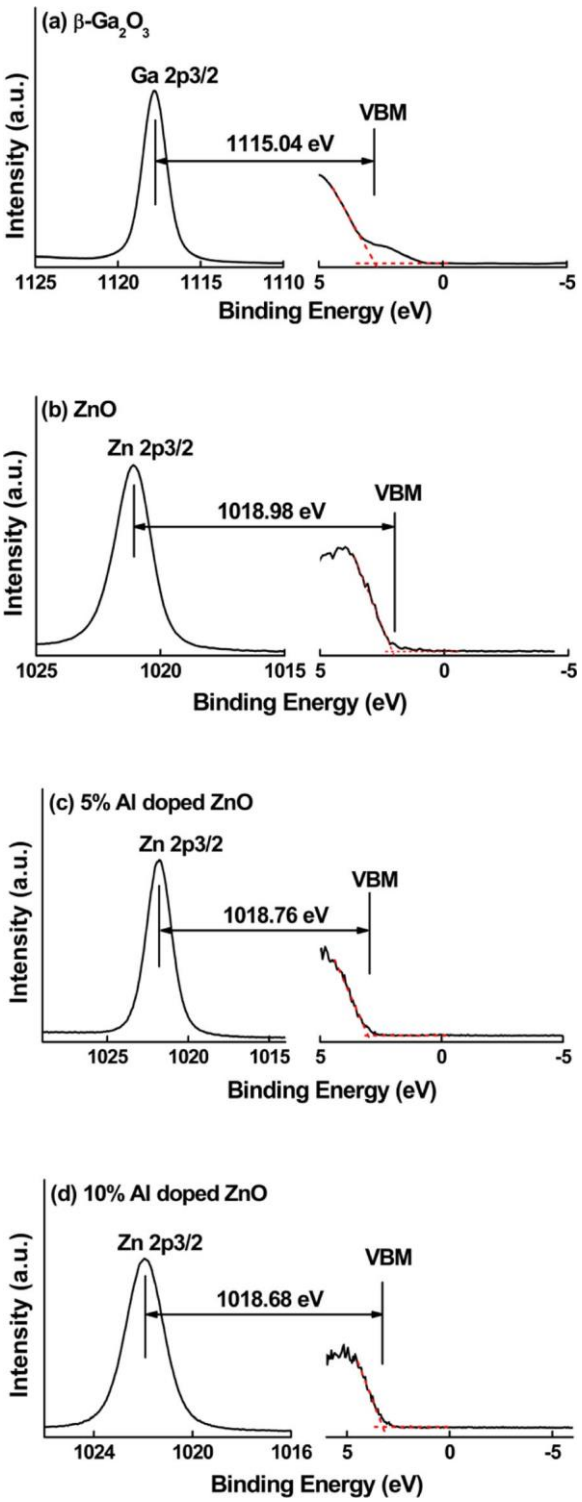

Fig. 1 High resolution XPS spectra for core level and valence band maximum (VBM) of a Ga 2p core level spectrum and VBM from bare β-Ga_2O_3, b Zn 2p core level spectrum and VBM from thick pure ZnO/β-Ga_2O_3, c Zn 2p core level spectrum and VBM from thick 5% Al-doped ZnO/β-Ga_2O_3, and d Zn 2p core level spectrum and VBM from thick 10% Al-doped ZnO/β-Ga_2O_3

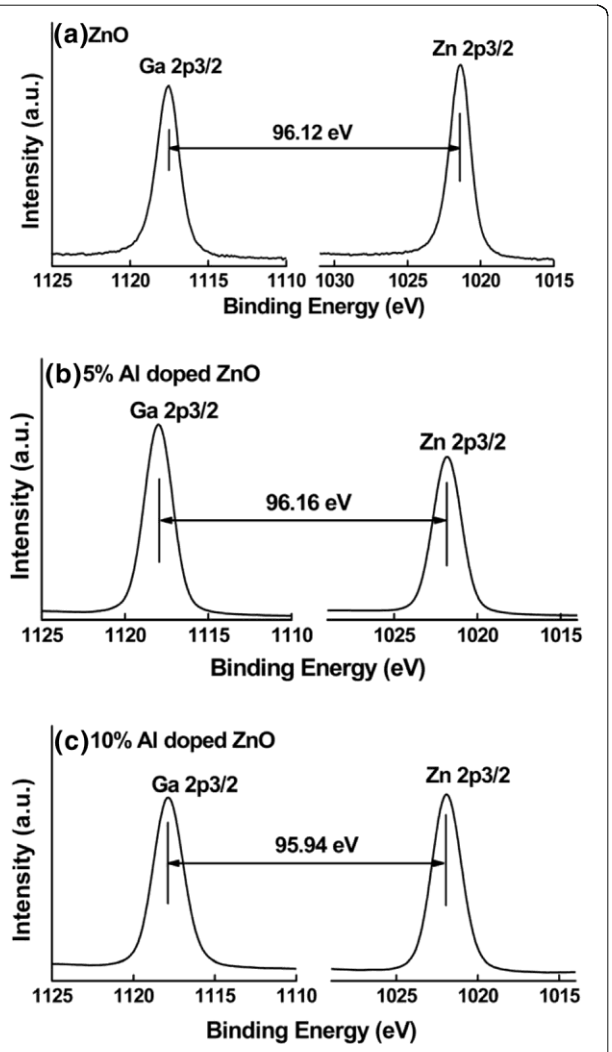

Fig. 2 The core level spectra of Ga 2p and Zn 2p obtained from high resolution XPS spectra of a thin ZnO/β-Ga_2O_3, b thin 5% Al-doped ZnO/β-Ga_2O_3, and c thin 10% Al-doped ZnO/β-Ga_2O_3

$E^{AZO}_{Zn\ 2p}$ refer to the BE of Ga 2p and Zn 2p CLs in thin Al-doped ZnO films, respectively.

Subsequently, based on the E_g and ΔE_V, the CBO at the Al-doped ZnO/β-Ga_2O_3 interface can be calculated by the following equation:

$$\Delta E_C = E_g^{Ga_2O_3} - E_g^{AZO} - \Delta E_V \quad (2)$$

where $E_g^{Ga_2O_3}$ is the bandgap of Ga_2O_3 and E_g^{AZO} is the bandgap of Al-doped ZnO. The bandgaps for undoped, 5% Al-doped ZnO, 10% Al-doped ZnO, and β-Ga_2O_3 are 3.20 eV, 3.25 eV, 3.40 eV, and 4.65 eV, respectively [17, 19]. The bandgap increases with a higher Al doping ratio, agreeing well with the simulation in the next part.

Figure 1 shows the Ga and Zn element CLs and VBM of bulk β-Ga_2O_3, thick undoped, and 5% and 10% Al-doped ZnO films. Fitting the linear area and the flat

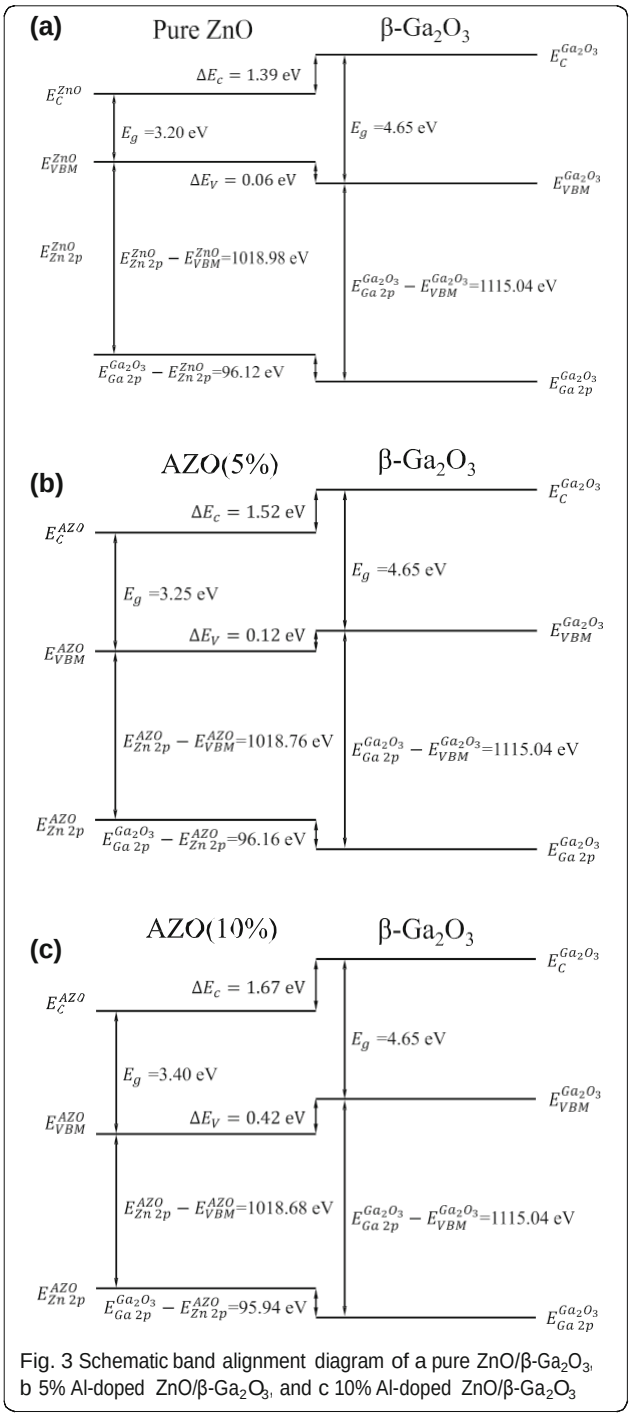

Fig. 3 Schematic band alignment diagram of a pure ZnO/β-Ga_2O_3, b 5% Al-doped ZnO/β-Ga_2O_3, and c 10% Al-doped ZnO/β-Ga_2O_3

band zone from the VBM spectrum can deduce the VBM [20]. Figure 2 shows Ga 2p and Zn 2p CL from various thin Al-doped ZnO/β-Ga_2O_3 heterojunctions. The BE differences of Ga 2p and Zn 2p CLs for the undoped, 5% Al-doped ZnO/β-Ga_2O_3, and 10% Al-doped ZnO/β-Ga_2O_3 are obtained to be 96.12 eV, 96.16 eV, and 95.94 eV, respectively. Then, the VBOs at the interfaces are determined to be 1.39 eV, 1.52 eV, and

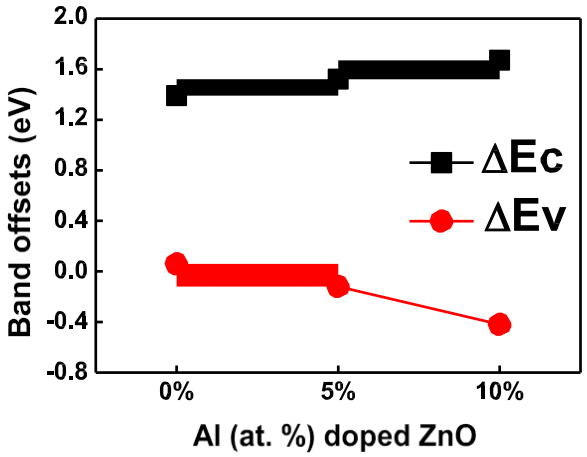

Fig. 4 The conduction and valence band offsets of atomic-layer-deposited AZO/β-Ga_2O_3 heterojunctions fabricated at different Al doping ratios

1.67 eV for the undoped, 5% Al-doped ZnO/β-Ga_2O_3, and 10% Al-doped ZnO/β-Ga_2O_3 samples, respectively.

The systematic band alignment for the 0%, 5%, and 10% Al-doped ZnO/β-Ga_2O_3 heterojunctions are calculated by the above equations, as shown in Fig. 3. The band offset of undoped ZnO/β-Ga_2O_3 heterojunction belongs to type I. While both 5% and 10% Al-doped ZnO/β-Ga_2O_3 heterojunctions have type-II band offsets. Figure 4 depicts the band alignments of Al-doped ZnO/β-Ga_2O_3 interfaces have a similar linear relationship with Al doping concentration. The CBO varies from 1.39 to 1.67 eV with the Al-doped concentration increasing from 0 to 10%. While the VBO reduces from 0.06 to − 0.42 eV with the Al-doped concentration rising from 0 to 10%. It is noted that the CBO and VBO for sputtered AZO/β-Ga_2O_3 are 0.79 eV and 0.61 eV, respectively [9]. Both the conduction and valence band shift downward in this work, which could be due to the different composition ratio and crystalline structure introduced by deposited methods.

Other than that, first-principle simulations were performed by the Vienna Ab-initio Simulation Package (VASP) [21–24] to investigate the electronic band structure and band alignment of Al-doped ZnO/Ga_2O_3 heterojunctions. During the calculation, the electron-ion interactions were treated by the ultra-soft pseudo-potentials, and the wave functions and potentials were expanded by the plane-wave basis [25].

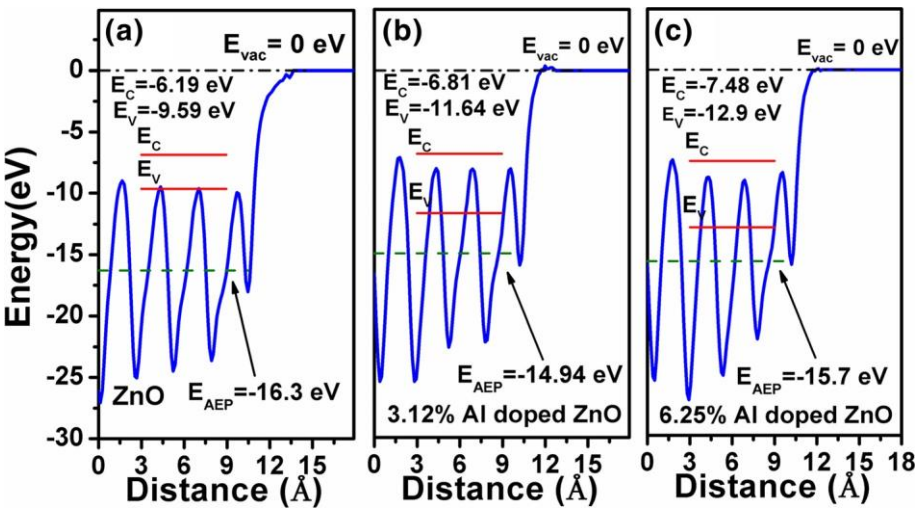

Fig. 5 The calculated band diagram of a undoped ZnO, b 3.21% Al-doped ZnO, and c 6.25% Al-doped ZnO structure. The Fermi levels were set to 0 eV

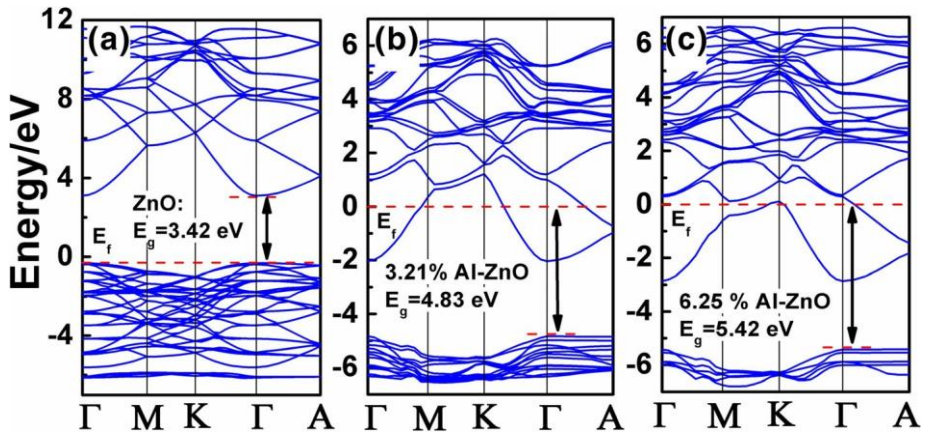

Fig. 6 The band alignment of AZO/β-Ga_2O_3 heterojunctions with a undoped, b 3.21%, and c 6.25% Al-doped ZnO. The vacuum levels were scaled to 0 eV

Besides, generalized gradient approximation (GGA) proposed by Perdew, Burke, and Ernzerhof (PBE) was implemented to describe the exchange-correlation energies [26]. Prior to initiating the simulation, converging tests were performed. It showed that the cutoff energy of 450 eV for the plane-wave basis and k-space grids of $3 \times 3 \times 3$ with the Monkhorst Pack scheme gave the well-converged results. In the structure optimization, a conjugate gradient method was used and the residual force was released until it was less than 0.01 eV/Å. Moreover, the hybrid density functions based on the semi-local PBE approximation were implemented. To correct the underestimated bandgap, 35% of PBE exchange was replaced with the exact one [27]. To identify the band edge shift with the change of the Al doping level, the average electrostatic potential (AEP) was calculated and aligned to the vacuum level which was scaled to 0 V. The VBM and conduction band minimum (CBM) were consequently aligned to the AEP based on the band diagram [28]. In this work, bulk ZnO with 16 O atoms and 16 Zn atoms in the supercell was used. To introduce the Al doping, one or two Zn atoms in the supercell were replaced by the Al atoms, creating the Al-doped structure with the doping concentration of 3.21% and 6.25 %, respectively.

Figure 5 a–c shows the calculated band diagrams of the undoped, 3.21% Al-doped ZnO, and 6.25% Al-doped ZnO structures, respectively. It clearly shows that ZnO is a direct bandgap semiconductor with the bandgap of 3.42 eV, and the CBM as well as the VBM was located at the Γ point of Brillouin zone. These theoretical simulation results match the experimental value quite well [29]. With the Al doping, it could be found that the Fermi levels shifted upwards into the conduction band, which converts the pure ZnO into an n-type semiconductor. In the meanwhile, the bandgaps also increased to 4.83 eV and 5.42 eV for 3.21% Al-doped ZnO and 6.25% Al-doped ZnO, respectively. Although the bandgaps here for the doped ZnO are higher than our experimental results; however, this could be ascribed to the neglecting of interfacial defect states as well as other crystal defects.

Figure 6 a–c presents the band alignments of undoped, 3.21% Al-doped ZnO, and 6.25% Al-doped ZnO to the vacuum level. For the conduction bands of the materials, due to the strong electron mixing between the Al and O element, it could be found that the energy level decreases from − 6.19 eV of the ZnO to − 6.81 eV for the 3.21% Al-doped ZnO (ΔE = 0.62 eV) and further decreases to − 7.48 eV for the 6.25% Al-doped ZnO (ΔE = 1.29 eV). In the meanwhile, due to the opening up of the bandgap, it also could be found that the valence band edge moves downwards from − 9.59 eV for the ZnO to − 11.64 eV for 3.21% Al-doped ZnO (ΔE = 2.05 eV) and − 12.9 eV for the 6.25% Al-doped ZnO (ΔE = 3.31 eV). In all, ascribed to the strong Al and O electron mixing, it could be understood that incorporating Al in the ZnO would open up the band gaps. Moreover, it would shift both the conduction band and valence band edge towards the lower energy level when aligned to the vacuum level.

Conclusions

In conclusion, the band alignments of different Al-doped ZnO/β-$Ga_2O_3(\bar{2}01)$ interfaces have been investigated by XPS. A type-I band alignment forms at the interface of ZnO/β-Ga_2O_3 heterojunction. While the AZO/β-Ga_2O_3 interface has a type-II band alignment. The CBOs vary from 1.39 to 1.67 eV and the

VBOs reduce from 0.06 to −0.42 eV with the Al-doped concentration rising from 0 to 10%. Moreover, the density function calculations show that band offsets change due to strong Al and O electron mixing when Al is incorporated into ZnO. These results suggest that the pure ZnO is a valid ISL to reduce the barrier height and promote the electron transport.

Abbreviations

AEP: Average electrostatic potential; ALD: Atomic layer deposition; BE: Binding energy; CBM: Conduction band minimum; CBO: Conduction band offset; CL: Core level; CLs: Core levels; CVD: Chemical vapor deposition; DEZ: Zn $(C_2H_5)_2$; Ga_2O_3: Gallium oxide; GaN: Gallium nitride; GGA: Generalized gradient approximation; ISL: Intermediate semiconductor layer; PBE: Perdew, Burke, and Ernzerhof; SiC: Silicon carbide; TMA: Trimethyaluminum; VASP: Vienna Ab initio Simulation Package; VBM: Valence band maximum; VBO: Valence band offset; XPS: X-ray spectroscopy; ZnO: Zinc oxide

Acknowledgements

The authors would like to acknowledge the financial support in part by the National Natural Science Foundation of China (Nos. 61774041, 61704095, and 61474027), in part by Guangdong Province Key Technologies Research and Development Program (No. 2019B010128001), and in part by Shanghai Science and Technology Innovation Program (No.19520711500).

Authors' Contributions

SMS conducted the extensive experiments and analyzed the data. CJG conducted the theoretical calculations. WJL and SJD supervised the project and wrote the manuscript. DAG helped to review and discuss the manuscript. All authors read and approved the final manuscript.

Availability of Data and Materials

The datasets supporting the conclusions of this manuscript are included within the manuscript.

Competing Interests

The authors declare that they have no competing interests.

Author details

[1]State Key Laboratory of ASIC and System, School of Microelectronics, Fudan University, Shanghai 200433, China. [2]Belarusian State University of Informatics and Radioelectronics, P. Brovka Street 6, 220013 Minsk, Belarus. [3]Division of Microelectronics, School of Science, Ningbo University, Ningbo 315211, China.

Received: 10 May 2019 Accepted: 17 July 2019
Published online: 14 August 2019

References

1. Mastro MA, Kuramata A, Calkins J, Kim J, Ren F, Peartong SJ (2017) Perspective: opportunities and future directions for Ga_2O_3. ECS J Solid State Sc 6(5):356–359
2. Si M, Yang L, Zhou H, Ye PD (2017) β-Ga_2O_3 Nanomembrane negative capacitance field-effect transistors with steep subthreshold slope for wide band gap logic applications. ACS Omege 2(10):7136–7140
3. Green AJ, Chabak KD, Heller ER, Fitch RC, Baldini M, Fiedler A et al (2016) 3. 8-MV/cm breakdown strength of MOVPE-grown Sn-doped β-Ga_2O_3 MOSFETs. IEEE Electron Device Lett 37(7):902–905
4. Moser NA, McCandless JP, Crespo A, Leedy KD, Green AJ, Heller ER, Chabak KD, Peixoto N, Jessen GH (2017) High pulsed current density β-Ga2O3 MOSFETs verified by an analytical model corrected for interface charge. Appl Phys Lett 110(4):143505
5. Sasaki K, Higashiwaki M, Kuramata A, Masui T, Yamakoshi S (2013) Si-ion implantation doping in β-Ga_2O_3 and its application to fabrication of low-resistance Ohmic contacts. Appl Phys Exp 6(4):086502
6. Higashiwaki M, Sasaki K, Kamimura T, Wong M, Krishnamurthy D, Kuramata A et al (2013) Depletion-mode Ga_2O_3 metal-oxide-semiconductor field-effect transistors on β-Ga_2O_3 (010) substrates and temperature dependence of their device characteristics. Appl Phys Lett 103(12):123511
7. Armstrong AM, Crawford MH, Jayawardena A, Ahyi A, Dhar S (2016) Role of self-trapped holes in the photoconductive gain of β-gallium oxide Schottky diodes. J Appl Phys 119(10):103102
8. Carey PH, Yang J, Ren F, Hays DC, Pearton SJ, Jang S et al (2017) Improvement of Ohmic contacts on Ga_2O_3 through use of ITO-interlayers. J Vac Sci Technol B 35(6):061201
9. Carey PH, Yang J, Ren F, Hays DC, Pearton SJ, Jang S et al (2017) Ohmic contacts on n-type β-Ga_2O_3 using AZO/Ti/Au. Aip Adv 7(9):095313
10. Qian X, Cao Y, Guo B, Zhai H, Li A (2013) Atomic layer deposition of Al-doped ZnO films using aluminum isopropoxide as the Al precursor. Chem Vapor Depos 19:180–185
11. Su YC, Chiou CC, Marinova V, Lin SH, Bozhinov N, Blagoev B, Babeva T, Hsu KY, Dimitrov DZ (2018) Atomic layer deposition prepared Al-doped ZnO for liquid crystal displays applications. Opt Quant Electron 50:205
12. Chauveau JM, Vennéguès P, Laügt M, Deparis C, Zuniga-Perez J, Morhain C (2008) Interface structure and anisotropic strain relaxation of nonpolar wurtzite $(11\bar{2}0)$ and $(10\bar{1}0)$ orientations: ZnO epilayers grown on sapphire. J Appl Phys 104:073535
13. Ellmer K, Kudella F, Mientus R, Schieck R, Fiechter S (1994) Influence of discharge parameters on the layer properties of reactive magnetron sputtered ZnO:Al films. Thin Solid Films 247(1):15–23
14. Kumar M, Mehra RM, Wakahara A, Ishida M, Yoshida A (2003) Epitaxial growth of high quality ZnO:Al film on silicon with a thinγ-Al_2O_3 buffer layer. J Appl Phys 93(7):3837–3843
15. Lee DJ, Kim HM, Kwon JY, Choi H, Kim SH, Kim KB (2011) Structural and electrical properties of atomic layer deposited Al-doped ZnO films. Adv Funct Mater 21(3):448–455
16. George SM (2010) Atomic layer deposition: an overview. Chem Rev 110(1):111–131
17. Liu WJ, Wang YH, Zheng LL, Lu HL, Ding SJ (2017) Stability enhancement of low temperature thin-film transistors with atomic-layer-deposited ZnO:Al channels. Microelectronic Engineering 167(5):105–109
18. Kraut EA, Grant RW, Waldrop JR, Kowalczyk SP (1980) Precise determination of the valence-band edge in X-ray photoemission spectra: application to measurement of semiconductor interface potentials. Phys Rev Lett 44(24):1620–1623
19. Sun SM, Liu WJ, Xiao YF, Huan YW, Liu H, Ding SJ, Zhang DW (2018) Investigation of energy band at atomic-layer-deposited ZnO/β-Ga_2O_3 $(\bar{2}01)$ heterojunctions. Nanoscale Res Lett 13:412
20. Carey PH IV, Ren F, Hays DC, Gila BP, Pearton SJ, Jang S, Kuramata A (2017) Valence and conduction band offsets in AZO/Ga_2O_3 heterostructures. Vacuum 141:103–108
21. Kresse G, Hafner J (1993) Ab initio molecular dynamics for liquid metals. Phys Rev B 47(1):558–561
22. Kresse G, Furthmüller J (1994) Ab initio molecular-dynamics simulation of the liquid metal amorphous semiconductor transition in germanium. Phys Rev B 49(20):14251–14269
23. Kresse G, Furthmüller J (1996) Efficiency of ab-initio total energy calculations for metals and semiconductors using a plane-wave basis set. Comput Mat Sci 6(1):15–50
24. Kresse G, Furthmüller J (1996) Efficient iterative schemes for ab initio total-energy calculations using a plane-wave basis set. Phys Rev B 54(16):11169–11186
25. Vanderbilt D (1990) Soft self-consistent pseudopotentials in a generalized eigenvalue formalism. Phys Rev B 41(11):7892
26. Perdew JP, Burke K, Ernzerhof M (1996) Generalized gradient approximation made simple. Phys Rev Lett 77(18):3865–3868
27. Broqvist P, Alkauskas A, Pasquarello A (2010) A hybrid functional scheme for defect levels and band alignments at semiconductor-oxide interfaces. Phys Status Solidi 207(2):270–276
28. Shi LB, Li MB, Xiu XM, Liu XY, Zhang KC, Liu YH, Li CR, Dong HK (2017) First principles calculations of the interface properties of a-Al_2O_3/MoS_2 and effects of biaxial strain. J Applied Phys 121:205305
29. Ozgure U, Alivov YI, Liu C, Teke A, Reshchikov MA, Dogan S, Avrutin V, Cho SJ, Morkoc H (2005) A comprehensive review of ZnO materials and devices. J Applied Phys 98:041301

Publisher's Note

Springer Nature remains neutral with regard to jurisdictional claims in published maps and institutional affiliations.